# A Study of Open Boundary Conditions for Far Field Tsunami Computation

MD. FAZLUL KARIM[a], G D ROY[b], AHMAD IZANI M ISMAIL[a]
[a] School of Mathematical Sciences, Universiti Sains Malaysia, 11800 Pulau Pinang, Malaysia
[b] Department of Mathematics, Shahjalal University of Science & Technology, Sylhet, Bangladesh

**mdfazlulkk@yahoo.com** ; gaurangadebroy@gmail.com; izani@cs.usm.my

**Abstract:** The lethal Indian Ocean tsunami of December 26, 2004 hit the southeast and south-Asian and east African countries causing devastation of undescribable properties. The wave reached the coast of Africa with considerable intensity traveling ~ 4500 km from the epicenter. The purpose of this study is to compute the effect of initial wave associated with a far field tsunami source in a region of interest within a limited area model. In order to simulate the far field tsunami, four model domains have been considered: these are the original domain (OD) which is same as Roy et al. (2006) and three extended domains ED(1), ED(2) and ED(3) obtained by extending the west boundary of OD through 1100, 1500 and 4500 km respectively. The source of Indonesian tsunami 2004 is shifted to each of the extended domains to compute its response along the western open boundary of OD. Using these data, the open boundary condition of Roy et al. (2006) is applied along the western boundary of OD for generating response along the west coast of Peninsular Malaysia and Thailand in absence of any source. It is found that by proper choice of the amplitude and scale factors associated with the boundary condition, it is possible to generate similar response of a far field tsunami source with reasonable accuracy.

*Key words*: Open boundary condition; Shallow water model; Far field tsunami; Indonesian tsunami 2004; Tsunami propagation and surge; damping amplitude.

## 1. Introduction

Tsunamis are a series of enormous waves created by an underwater disturbance such as an earthquake, landslide, volcanic eruption, or meteorite. Tsunami waves can be generated when the sea floor abruptly deforms and vertically displaces the overlying water. A tsunami can move at hundreds of kilometers per hour in the open ocean and may smash into land with waves as high as 30 meters or more. A tsunami can have a wavelength in excess of 100 km and period in the range of 10 min to one hour. Tsunamis are called local, regional and distant if the distances of the source are within 100 km, 100–700 km, and more than 700 km respectively from the coast.

As a result of their long wave lengths, tsunamis behave as shallow-water waves. A wave becomes a shallow-water wave when the ratio between the water depth and its wave length gets very small (< 0.05). Shallow-water waves move at a speed that is equal to the square root of the product of the gravity acceleration and the water depth. Because the rate at which a wave losses its energy is inversely related to its wave length, tsunamis not only propagate at high speeds, but also they can travel great transoceanic distances with limited energy losses.

Numerical simulations of tsunami propagation have greatly improved in the last 30 years. Several computational models are being used in the National Tsunami Hazard Mitigation Program, sponsored by the National Oceanic and Atmospheric Administration (NOAA). The computational models include MOST (method of splitting tsunami), developed originally by researchers at the University of Southern California (Titov and Synolakis, 1998) and TUNAMI, developed at Tohoko University in Japan (Imamura, 1996). Kowalik et al. (2005) developed a global model to simulate the generation, propagation and run-up of the tsunami associated with the 26 December 2004

Manuscript received Sep. 14, 2007; revised Mar. 20, 2008


event throughout the globe between 80° S and 69° N. A nonlinear Polar coordinate shallow water model has recently been developed by Roy et al. (2006) to compute the effect of Indonesian tsunami 2004 along the west coast of Peninsular Malaysia and North Sumatra. All of these models require further validation by large-scale laboratory experiments and/or field data. A series of studies on tsunami computation have been performed all over the world. Some of these are the studies of Kowalik and Whitmore (1991), Kienle et al. (1996), Imamura and Gica (1996), Titov and Gonzalez (1997), Imteaz and Imamura (2001), Zahibo et al. (2003a), Zahibo et al. (2003b), Roy and Ismail (2005).

In the past two decades, several works for estimating far field tsunami have emerged in the literature (see, e.g., Go et al. 1988; Nagano et al. 1991; Mofjeld et al. 2001; Koike et al. 2003). They have used some historical data to assess the tsunami risk for coastal locations in the Caribbean Sea. All of these studies are very popular for estimations of far field tsunami potentials when the tsunami sources are located in the open sea. Zahibo et al. (2003a) has estimated far field tsunami potential for the Caribbean coast based on the numerical simulation of the few prognostic events using TUNAMI2. They have used some events using the known characteristics of their origin (coordinate, magnitude etc) and estimated their effects in five selected zones.

The response of initial tsunami waves generated at any location can reach every distant corner (Kowalik et al. 2005). So it is necessary to estimate the response along a particular region of interest due to a tsunami source located far away from that region. This may be done through a global model that contains both the source region and the region of interest. But a global model is very expensive in terms of both computer storage and CPU time and is not suitable for real time simulation. The alternative is to incorporate appropriate boundary conditions in a limited area model surrounding the region of interest.

In general, an open boundary condition is used to ensure transparency in allowing disturbances created in a model domain to go out. This may as well be used to allow disturbances to enter transparently from outside into the model domain. For example, tidal oscillation in a limited area model domain is generated through this method (Johns et al. 1985, Roy 1995). A sinusoidal wave is allowed to propagate into the model domain through an open boundary by using appropriate amplitude, phase and time period of the wave. The response of this type of boundary condition at every grid point is also sinusoidal. By adjusting the amplitude and phase it is possible to generate a representative tidal oscillation of specific time period in the model domain. Similarly, in computing the effect of far field tsunami source in a limited area model, a boundary condition may be incorporated along the open boundary, which is facing the tsunami source.

A nonlinear Cartesian coordinate shallow water model was developed by Roy and Ismail (2005) to compute the effect of the 2004 tsunami along the west coast of Peninsular Malaysia and Thailand associated with the Indonesian tsunami 2004. The analysis area of this model is a rectangular region approximately between 2–14° N and 91–101.5° E. The model area includes the source region of 2004 event. The model of Roy and Ismail (2005) is used to formulate a boundary condition along the western open boundary, parallel to *y*-axis, so that its response along the west coast of Peninsular Malaysia and Thailand agrees reasonably well with the observed data of 2004 tsunami (Roy et al. 2006). The following procedure was adopted to search for the desired boundary condition:

The model of Roy and Ismail (2005), with governing equations and boundary conditions, was applied to compute the maximum amplitudes and time series of water levels along the western open boundary associated with the source of Indonesian tsunami 2004. Based on these data, Roy et al. (2006) formulated a boundary condition along this open boundary. This formulated boundary condition was applied to compute the effect of tsunami in the absence of any source in the model domain.

The limitation of the study of Roy et al. (2006) lies in the fact that the response along the western open boundary has been computed due

Manuscript received Sep. 14, 2007; revised Mar. 20, 2008


to the source which is inside the model domain. But for developing appropriate boundary condition due to far field tsunami, the response data along the open boundary must be obtained due to sources outside the model domain. In the present study, to compute the affects of far field tsunami along the coastal belts of Phuket and Penang Island, four domains have been considered: one is the original domain similar to that of Roy and Ismail (2005), abbreviated as OD. The other three extended domains, abbreviated as ED(1), ED(2) and ED(3), are obtained by placing the western open boundary 1100 km, 1500 km and 4500 km away from the open boundary of OD. This is done to facilitate shifting of the position of the source of Indonesian tsunami 2004 outside OD. Setting this source in every ED(*i*) we investigate its response along the west open boundary of OD. Based on these responses, a boundary condition similar to Roy et al. (2006) has been used for the western open boundary of OD to compute the effects of far field tsunami along Phuket and Penang in absence of any source (Fig.1).

## 2. Mathematical Formulation

### 2.1. *Depth averaged shallow water equations*

The depth averaged equations are as follows:

$$\frac{\partial \zeta}{\partial t} + \frac{\partial}{\partial x}\left[(\zeta + h)u\right] + \frac{\partial}{\partial y}\left[(\zeta + h)v\right] = 0 \quad (1)$$

$$\frac{\partial u}{\partial t} + u\frac{\partial u}{\partial x} + v\frac{\partial u}{\partial y} - fv = -g\frac{\partial \zeta}{\partial x} - \frac{C_f u\left(u^2 + v^2\right)^{1/2}}{(\zeta + h)} \quad (2)$$

$$\frac{\partial v}{\partial t} + u\frac{\partial v}{\partial x} + v\frac{\partial v}{\partial y} + fu = -g\frac{\partial \zeta}{\partial y} - \frac{C_f v\left(u^2 + v^2\right)^{1/2}}{(\zeta + h)} \quad (3)$$

Here $u$ and $v$ are the $x$ and $y$ components of velocity of sea water respectively, g is gravity, $f$ is Coriolis parameter, $\zeta$ is the displacement of the free surface from the equilibrium state, $C_f$ is the bottom friction coefficient, $h$ is ocean depth from the mean sea level.

### 2.2. *Model domain and boundary conditions*

In the introduction we have discussed about original domain (OD) and the extended domains ED(*i*), *i* = 1, 2, 3. The OD is a rectangular region that lies between 2°–14° N and 91°–101.5° E. This model area includes the source region of the Indonesian tsunami 2004.

Other than the west coast of Peninsular Malaysia and Thailand, the boundaries are considered as straight lines in the sea. The southern and northern open sea boundaries lie parallel to $x$-axis and the western open sea boundary lies parallel to $y$-axis. For each ED(*i*), following Roy (1995), the radiation boundary conditions for the west, south and north open sea boundaries are

$u - (g/h)^{1/2}\zeta = 0$ at the west boundary; parallel to $y$-axis (4)

$v + (g/h)^{1/2}\zeta = 0$ at the south boundary; along $x$-axis (5)

$v - (g/h)^{1/2}\zeta = 0$ at the north boundary; parallel to $x$-axis (6)

This type of boundary condition allows the disturbance, generated within the model area, to go out through the open boundary. For the OD, the southern and northern open boundary conditions are also given by (5) and (6). The western open boundary conditions of OD will be discussed later. The coastal belts of the mainland and islands are the closed boundaries where the normal components of the velocities are taken as zero.

## 3. Numerical Method

### 3.1. *Grid Generation*

Manuscript received Sep. 14, 2007; revised Mar. 20, 2008


A rectangular grid system is generated in the analysis area using a set of equidistant straight lines parallel to the *x*-axis and a set of equidistant straight lines parallel to the *y*-axis. The space between any two consecutive gridlines parallel to the *y*-axis is $\Delta x$ and that between any two consecutive gridlines parallel to the *x*-axis is $\Delta y$. Let there be *M* gridlines parallel to *y*-axis and *N* gridlines parallel to the *x*-axis so that the total number of grid points are $M \times N$. We define the grid points $(x_i, y_j)$ in the domain by

$$x_i = (i-1)\Delta x, \qquad i = 1, 2, 3, \ldots, M \quad (7)$$

$$y_j = (j-1)\Delta y, \qquad j = 1, 2, 3, \ldots, N \quad (8)$$

The sequence of discrete time instants is given by

$$t_k = k\,\Delta t, \qquad k = 1, 2, 3, \ldots \quad (9)$$

3.2. *Numerical Scheme and Model Data Set-up*

The governing equations (1)–(3) together with the boundary conditions (4)-(6) are discretized by finite difference (forward in time and central in space) and are solved by a conditionally stable semi-implicit method using a staggered grid system which is similar to the Arakawa C system.

The origin of the Cartesian coordinate system is at *O* (3.125° N, 101.5° E), the *x*-axis is directed towards west at an angle 15° (anticlockwise) with the latitude line through *O* and the *y*-axis is directed towards north inclined at an angle 15° (anticlockwise) with the longitude line through *O*. The analysis area is a rectangular region between 2–14° N and 91–101.5° E (Fig.1). The model area of OD includes the source region of Indonesian tsunami 2004. The number of grids in *x*-direction and *y*-direction are respectively *M* = 230 and *N* = 319 so that there are 73370 grid points in the computational domain of OD. The number of grids for ED(1), ED(2), and ED(3) are 500 ×319, 650 × 319, and 1400 × 319 respectively. The grid size of the rectangular mesh is given by $\Delta x = \Delta y$ = 4 km for all the model areas. The time step $\Delta t$ is taken as 10 seconds which satisfies the CFL criterion and thus ensures the stability of the numerical scheme. Following Kowalik et al. (2005), the value of the friction coefficient $C_f$ is taken as 0.0033 through out the model area. The depth data for OD are collected from the Admiralty bathymetric charts and at the extended part of every ED(*i*), an average depth is used (3000 m).

## 4. Initial condition (Tsunami Source Generation)

The generation mechanism of the 26 December 2004 tsunami was mainly due a static sea floor deformation caused by an abrupt slip at the India/Burma plate interface. The extent of the rupture is estimated to be 1200–1400 km from the epicenter along the fault line (Amon et al. 2005, Hirata et al. 2006, Ohta et al. 2006, Tanioka et al. 2006). According to the estimation, the tsunami source is extended along the fault from south-east to north-west with uplift to subsidence from west to east. According to the supporting online materials of Amon et al. (2005) Fig. S2, the extent of the rupture zone is between 92–97° E and 2–13° N with maximum uplift to subsidence of the sea bed within ± 5 m; the intensity of uplift/subsidence is least in the region 2–13° N . Tanioka et al. (2006) computed the rupture zone between 92–97° E and 2–13.5° N; the estimated subsidence to uplift is within –3 to 8 m. According to Kowalik et. al. (2005), the computed rupture zone is 92–97°E and 3–11°N with a maximum uplift of 507 cm at the west and maximum subsidence of 474 cm at the east. Based on the above information we consider that the source of Indonesian tsunami 2004 as extending along the fault line between 92–97° E and 2–13.5° N with a maximum rise of 5 m and maximum fall of 4.75 m of the sea surface. Relative to the west coast of Malaysia and Thailand, the source is in the form of sea level trough to crest. The disturbance in the form of rise and fall of sea surface is assigned as the initial condition with a maximum rise of 5 m to maximum fall of 4.75 m.

To compute the far field tsunami along the west coast of Thailand and Peninsular Malaysia we set the source in ED(1), ED(2), and ED(3) by shifting the position of the Indonesian tsunami 2004 source through 1100, 1500 and 4500 km

Manuscript received Sep. 14, 2007; revised Mar. 20, 2008


respectively without altering its intensity and orientation.

## 5. Effects of far field tsunami

To investigate the effects of the far field tsunami along the west coast of Thailand and Peninsular Malaysia we compute response of the source placed in every ED(*i*), as mentioned in a previous section.

### 5.1. *Propagation of tsunami generated through far field tsunami source*

The propagation of the tsunami waves, generated by the source at ED(1), along with the arrival times at the coasts has been computed. Figure 2 shows the time, in minutes, for attaining +0.1 m sea level rise at each grid point in the model domain. Thus considering the 0.1 m sea level rise as the arrival of tsunami, it is seen that, the disturbance propagates gradually towards the coast (Fig. 2). The arrival times of the waves at Phuket and Penang are respectively 210 min and 350 min. On the other hand, by placing the source in its original position in OD, the arrival time of tsunami at Phuket and Penang are respectively 90 min and 230 min, which are consistent with the data available in USGS website. Since the position of the source in ED(1) is 1100 km away from its original position, the arrival of waves at the coastal belts is delayed by 120 min.

The propagation of the tsunami waves, generated by the sources in ED(2) and ED(3) has also been computed. Due to the source in ED(2) the arrival time of the wave at Phuket and Penang are 250 min and 400 min respectively. Due to the source in ED(3), the arrival times are 550 min and 700 min respectively (not shown).

### 5.2. *Maximum water level due to far field tsunami source*

Figure 3 depicts the maximum water level along the peninsular west coast from Penang Island to Phuket due to the source in ED(1). The surge amplitude is increasing from south to north; the maximum water level attained is 12.09 m and around Phuket the maximum water level is 4.03–10.48 m. On the other hand, the maximum water level around Penang Island is 1.6–3.2 m. From the contour plot it is seen that, the surge amplitude is increasing very fast near the shoreline everywhere (Fig. 3).

Maximum water levels along the west coast from Penang Island to Phuket due to the sources in ED(2) and ED(3)- are found to be 11.82 m and 8.87 m (not shown). Thus the maximum surge level is decreasing with the increase of the distance of the source position from the west coast.

### 5.3. *Water levels at Phuket and Penang due to far field tsunami source*

The fluctuation of water levels with respect to time at Phuket due to the initial tsunami wave generated at the source in ED(1) is shown in Fig. 4. At the east coast of Phuket, the water level is oscillatory with a maximum level of 4.7 m and the oscillation continues with damping amplitude (Fig. 4a). In fact, 3.0 h after generation of the initial tsunami wave, the water level starts decreasing and reaches a minimum level of –1.8 m. Then it increases continuously to reach 4.7 m at 3.75 h before going down again. At the south-west coast of Phuket the time series is also oscillatory with minimum of – 4.0 m and the maximum up to 7.8 m and the oscillation continues with damping amplitude (Fig. 4b).

Figure 5 shows a similar fluctuation at north and south coasts of Penang Island. At Batu Ferringi (north coast) the maximum elevation is approximately 3.2 m (Fig. 5a); 5 hrs after the generation of initial wave due to source in ED(1), the water level starts decreasing and reaches to the level –0.9 m and then the water level increases continuously to reach a level of 3.2m ($1^{st}$ crest) at 5 hrs 20 min before going down again. At the south coast the time series is also oscillatory with maximum elevation of 2.0 m (Fig. 5b).

For the other two far field sources at ED(2) and ED(3), the computed water levels are also of similar patterns as those due to source in ED(1) (not shown).

Manuscript received Sep. 14, 2007; revised Mar. 20, 2008


## 6. Tsunami Computation through an Open Boundary Condition

### 6.1. *Open boundary condition in OD*

In order to incorporate an open boundary condition in OD for computing the effect of far field tsunami sources, we first investigated the response of the sources in ED(1), ED(2) and ED(3) along the western open boundary of OD. Figure 6 shows the maximum amplitudes of tsunami waves along the west open boundary of OD due to the sources in ED(*i*). Solid, dash-dotted and dotted lines show the amplitudes due to sources in ED(1), ED(2) and ED(3) respectively. It is evident that, the amplitude of the wave decreases with increasing distance of the source position from the boundary. Figure 7 shows the time series at a point of the west open boundary of OD due to the above sources; and these are found to be oscillatory with damping amplitude.

For generating tidal oscillation in a limited area model through an open boundary, generally the formulation is done by associating a sinusoidal term, containing amplitude, period and phase, with the open boundary condition (Johns et al. 1985, Roy 1995). The amplitude of this sinusoidal term at a particular point of the boundary remains, in general, constant with respect to time. In case of tsunami propagation, the time series at a particular point is also oscillatory but with damping amplitude. On the basis of the information in Figs. 6 and 7, following Roy et al. (2006), an open boundary condition at the west boundary (parallel to *y*-axis) of OD is given by

$$u - \sqrt{g/h}\,\zeta = -2\sqrt{g/h}\,e^{-st}a\sin(2\pi t/T + \varphi) \quad (10)$$

where $a$ is the amplitude, $T$ is the period, $\varphi$ is the phase of the wave and $s$ is the scale factor used for damping the amplitude of the wave with respect to time. In Eq. (14), the following conditions are imposed:

$$\begin{aligned} & s = 0 \quad \text{for} \quad t \le T \\ \text{and} \quad & s > 0 \quad \text{for} \quad t > T. \end{aligned} \quad (11)$$

Through the condition (11) we are allowing one wave, with full amplitude, to enter into the domain before damping of the amplitude begins. In Eq. (10), we have taken $\varphi = 0$, $T = 0.5$ h and $s = 0.01$ and the values of $a$ are taken according to those obtained in Fig. 6.

The boundary condition (10) at the western open boundary of OD, along with the values of $a$ (in Fig. 6) that are obtained along this boundary as the response of the source in ED(1), will henceforth be abbreviated as BC-ED(1). Similarly, BC-ED(2) and BC-ED(3) are the boundary conditions given by Eq. (14), along with the values of $a$ that are obtained as the responses of sources in ED(2) and ED(3) respectively.

### 6.2. *Tsunami propagation in the Phuket and Penang*

Results from the numerical simulation of the propagation of tsunami towards the west coast of Peninsular Thailand and Malaysia generated through the BC-ED(1) are shown in Figure 8. The propagation of incoming tsunami at the west coasts of Southern Thailand and Malaysia between Phuket in Thailand and Penang in Malaysia are investigated. The disturbance pattern of the sea surface is presented at four different instants of time. The wave celerity $c = \sqrt{g.h}$ near Phuket with water depths of about $h$ = 200 to 300 *m* is much higher than near the Penang region with water depths in between $h$ = 50 to 100 *m*. This results in a spreading of the incoming tsunami wave including a decrease of the wave height (time t = 3 to 4.5 hr). At 1.5 hr after the generation of the initial tsunami wave at the source, the sea surface disturbance is found to be proceeding towards Phuket with a trough at the front followed by a crest (Fig. 8a) and hits the Phuket coast at 2 hr after the generation. The wave is now propagating towards the Penang Island after flooding the Phuket region (Fig. 8b). In 3.5 hr the disturbance propagates further towards Penang Island and finally at 4.7 hr the tsunami surge is hitting the north and west coasts of Penang Island (Fig. 8c, d).

### 6.3. *Tsunami travel time*

Manuscript received Sep. 14, 2007; revised Mar. 20, 2008


Figure 9 shows the time, in minutes, for attaining +0.1 m sea level rise at each grid point generated through the BC-ED(1). The disturbance, created through the open boundary of OD, propagates gradually towards the coast and the arrival times of the wave at Phuket and Penang are 130 min and 280 min respectively. The arrival times of the waves at Phuket and Penang due to the disturbance created through each of BC-ED(2) and BC-ED(3) are identical with those due to the disturbance created through BC-ED(1).

### 6.4. *Maximum water level due to boundary conditions*

Figure 10 depicts the maximum water level along the Peninsular west coast from Penang Island to Phuket due to the waves generated through BC-ED(1). The surge amplitude is increasing from south to north; the highest water level attained is 14.15 m. The maximum water level surrounding Phuket is 4.7–11.3 m and the highest water level around Penang Island is 1.8–3.7 m. The surge amplitude due to BC-ED(1) is found to be more than that associated with the source in ED(1). The maximum water levels along the Peninsular west coast due to the waves generated through BC-ED(2) and BC-ED(3) reached up to 14.01 m and 13.36 m (not shown) respectively. The surge amplitudes due to BC-ED(2) and BC-ED(3) are found to be more than those associated with the sources in ED(2) and ED(3) respectively. Thus in every case the surge amplitude is found to be more due to the boundary condition than that generated through corresponding far field tsunami source.

### 6.5. *Water levels at Phuket and Penang Island due to boundary conditions*

The computed time series of surface fluctuation at Phuket and Penang Island as the response of the BC-ED(1) are shown in Figs. 11 and 12. At the east coast of Phuket the fluctuation begins with recession and 1.75 h after imposition of the boundary condition the water level reaches a minimum of –2.8 m; then it increases continuously to reach a maximum of 5.0m after 2.75 h and the fluctuation continues with damping amplitude (Fig. 11a). At the south-west coast of Phuket the fluctuation is also oscillatory; the minimum and maximum levels attained are –6.2 m and 7.2 m respectively and the oscillation continues with low amplitudes (Fig. 11b).

Figure 11 shows the fluctuation at the north and south coasts of Penang Island. At Batu Ferringi (north coast) the maximum elevation is approximately 4.8m (Fig. 12a). At 3.5 h after imposition of the boundary condition, the water level starts decreasing and reaches a minimum level of –1.6 m. Then the water level increases continuously to reach a level of 3.6m ($1^{st}$ crest) at 3 h 40 min before going down again. The water level oscillates and this oscillation continues for several hours with damping amplitude. At the south coast the fluctuation is also oscillatory and the maximum elevation is approximately 2.0 m (Fig. 12b). The time series of water levels at those locations associated with BC-ED(2) and BC-ED(3) are also found to be of similar pattern.

## 7. Adjustment of the Amplitude of the Boundary Condition

As mentioned earlier, the values of $a$ in BC-ED($i$) along the western open boundary of OD have been assigned from the set of data obtained as the response of the source placed in ED($i$). The intensity of water level due to every BC-ED($i$) is more than that generated through the corresponding far field tsunami source in ED($i$). To obtain the identical response through the boundary condition, we adjust the amplitude, $a$, in Eq. (10) by trial and error. It is found that, the amplitude $a$ (Fig. 6) in each of BC-ED(1) and BC-ED(2) needs to be multiplied by 0.85 and that of BC-ED(3), needs to be multiplied by 0.7. Thus the amplitude, $a$, in each of BC-ED(1) and BC-ED(2) is replaced by a new amplitude $a' = 0.85\ a$ and in BC-ED(3) by $a' = 0.7\ a$ to compute the response along the coastal belt.

### 7.1. *Maximum water level due to boundary condition with adjusted amplitude*

Figure 13 depicts the maximum water level associated with the adjusted BC-ED(1) along the peninsular west coast; the highest of maximum level is 12.26 m. The maximum water level surrounding Phuket is 3.6–9.8 m and the

Manuscript received Sep. 14, 2007; revised Mar. 20, 2008


maximum water level around Penang Island is 1.6–2.5 m. As mentioned earlier the highest of maximum level is 12.09 m and the maximum levels around Phuket and Penang Island are 4.03–10.48 m and 1.6–3.2 m associated with the response generated through the source in ED(1) (Fig. 3, section 5.2). The highest of maximum levels along the coastal belt associated with adjusted BC-ED(2), and BC-ED(3) are 11.85 m and 9.26 m respectively (not shown). These values are almost the same as the corresponding levels (11.82 m and 8.87 m) associated with the sources in ED(2) and ED(3) respectively (section 5.2). Thus, by proper choice of the value of the scale factor for the amplitude of the boundary condition, it may be possible to compute far field tsunami effect. The computed results for maximum water level along the peninsular west coast are summarized in Table 1. From this table it is evident that the computed maximum water levels due to adjusted BC-ED($i$) compares reasonably well with those due to corresponding sources in ED($i$).

For adjusting the water level due to every BC-ED($i$) with that due to the source in the corresponding ED($i$), we have replaced the amplitude $a$ by a new amplitude $a' = s' a$, where $s'$ is a scale factor. We have seen that for BC-ED(1-2), $s' = 0.85$ and for BC-ED(3), $s' = 0.7$. To investigate the quantitative nature of $s'$, we have conducted experiments by placing the source at some more extended domains. The values of the scale factor of the amplitude of the boundary condition in OD corresponding to response of the sources in different extended domains are shown in Table2.

7.2. *Anomaly of water level due to far field tsunami source and tsunami boundary condition*

Figure 14 shows the anomalies (difference) of maximum water levels generated through the source in ED(1) and due to BC-ED(1). Solid lines show the positive values and dashed lines show the negative values; the regions without contour lines have zero level. The difference of the maximum water levels is from -1 to +1.5 m only. From this contour plot it is evident that, other than the region surrounding Phuket, where the anomaly is nonzero, both results are identical. In the region surrounding Phuket the anomaly appears to be within tolerance level. The anomalies of maximum water levels generated through the source in ED(2) and due to BC-ED(2); are in the range -1.5– 2.5 m and the anomalies of the maximum water levels due to source in ED(3) and BC-ED(3) are in the range of -1.0–2.2 m (not shown in the figure). From these results it is evident that by proper choice boundary condition it is possible to compute far field tsunami within a reasonable accuracy.

## 8. Conclusion

In this paper, a shallow water nonlinear Cartesian coordinate model is used to compute the effects of far field tsunami in a limited area model using an appropriate boundary condition. For that purpose we have shifted the source of Indonesian tsunami 2004 to ~1100, 1500, and 4500 km away from the west coast of the original model domain with the same intensity and orientation of the source. By proper choice of the value of the scale factor, an open boundary condition has been formulated whose response in the model domain is reasonably consistent with the response of Indonesian tsunami 2004 situated far away from the fault zone. Thus, by choosing an appropriate open boundary condition it is possible to generate the response of a far field tsunami source with reasonable accuracy.

## Acknowledgements

This research is supported by FRGS, Federal Government Administrative Centre, 62505 Putrajaya, Malaysia and the authors acknowledge the support.

## References

[1] Ammon, J.C., Ji, C., Thio, H., Robinson, D., Ni, S., Hjorleifsdottir, V., Kanamori, H., Lay, T., Das, S., Helmberger, D., Ichinose, G., Polet, J., Wald, D., 2005. Rupture Process of the 2004 Sumatra-Andaman Earthquake. Science 308, 1133–1139.

[2] Go, Ch. N., Kaistrenko, V. M., Pelinovsky, E. N., Simonov, K. V., 1988. A quantitative estimation of tsunami hazard and the tsunami zoning scheme of the pacific coast of the USSR. Pacific Annual, Vladivostok 7–15.

[3] Hirata, K., Satake, K., Tanioka, Y., Kuragano, T., Hasegawa, Y., Hayashi, Y., Hamada, N., 2006. The 2004 Indian Ocean tsunami: Tsunami source model from satellite altimetry. Earth Planets Space 58, 195–201.

[4] Imamura, F., 1996. Simulation of wave-packet propagation along sloping beach by TUNAMI-code. Long-Wave Runup Models, World Scientific, 231–241.

[5] Imamura, F., Gica, E. C., 1996. Numerical Model for Tsunami Generation due to Subaqueous Landslide Along a Coast –A case study of the 1992 Flores tsunami, Indonesia. Sc. Tsunami Hazards. 14(1), 13 – 28.

[6] Imteaz, M. A., Imamura, F., 2001. A Non-Linear Numerical Model for Stratified Tsunami Waves and its Application. Sc. of Tsunami Hazards 19(3), 150–159.

[7] Johns, B., Rao, A.D., Dube, S. K., Sinha, P.C., 1985. Numerical modeling of the tide surges interaction in the Bay of Bengal. Phil. Trans. R. Sco. London, A 313, 507–535.

[8] Kienle, J., Kowalik, Z., Troshina, Elen, 1996. Propagation and Runup of Tsunami Waves Generated by Mt. St. Augustine Volcano, Alaska. Sc. Tsunami Hazards. 14(3), 191–206.

[9] Koike, N., Kawata, Y., Imamura, F., 2003. Far-field tsunami potential and a real time forecast system for the pacific using the inversion method. Natural Hazards 29, 423–436.

[10] Kowalik, Z., Whitmore, P. M., 1991. An Investigation of Two Tsunamis Recorded at Adak, Alaska. Sc. Tsunami Hazards. 9, 67 – 83.

[11] Kowalik, Z., Knight, W., Logan, T., Whitmore, P., 2005. Numerical Modeling of The Global Tsunami: Indonesian tsunami of 26 December 2004. Sc. of Tsunami Hazards, 23(1), 40–56.

[12] Mofjeld, H. O., Titov, V. V., Gonzalez, F. I., Newman, J. C., 2001. Tsunami scattering provinces in the Pacific Ocean. Geophysics Research Letters 28, 335–337.

[13] Nagano, O., Imamura, F., Shuto, N., 1991. A numerical model for a far-field tsunamis and its application to predict damages done to aquaculture. Natural Hazards 4, 235–255.

[14] Ohta, Y., Meilano, I., Sagiya, T., Kimata, F., Hirahara, K., 2006. Large surface wave of the 2004 Sumatra-Andaman earthquake captured by the very long baseline kinematic analysis of 1-Hz GPS data. Earth Planets Space 58, 153–157.

[15] Roy, G. D., 1995. Estimation of expected maximum possible water level along the Meghna estuary using a tide and surge interaction model. Environment International, 21(5), 671–677.

[16] Roy, G. D., Ismail, A.I.M., 2005. An investigation on the propagation of 26 December 2004 tsunami waves towards the west coast of Malaysia and Thailand using a Cartesian coordinates shallow water model. Proc. Int. Conf. in Mathematics and Applications. Mahidol University, Thailand, pp. 389–410.

[17] Roy, G.D., Karim, M. F., Ismail, A. M. I. 2006. Formulation of an Open Boundary Condition to Compute the Effect of Far Field Tsunami in the Domain of a Cartesian Coordinates Shallow Water Model, Far East Journal of Applied Mathematics 25(3), 253–272.

[18] Tanioka, Y., Yudhicara, Kususose, T., Kathiroli, S., Nishimura, Y., Iwasaki, S. I., Satake, K., 2006. Rupture process of the 2004 great Sumatra-Andaman earthquake estimated from tsunami waveforms. Earth Planets Space 58, 203–209.

[19] Titov, V. V., Gonzalez, F. I., 1997. Implementation and Testing of the Method of Spliting Tsunami (MOST) Model. NOAA Technical Memorandum ERL, PMEL -112, Contribution No. 1927 from NOAA/Pacific Marine Env. Lab. pp 11.

[20] Titov, V.V., Synolakis. C.E., 1998. Numerical modeling of tidal wave runup. Journal of Waterway, Port, Coastal and Ocean Engineering 124(4): 157–171.

[21] Zahibo, N., Pelinovsky, E., Kurkin, A., Kozelkov, A., 2003a. Estimation of far-field tsunami potential for the Caribbean coast based on numerical simulation. Sc. Tsunami Hazards 21(4) 202–222.

[22] Zahibo, N., Pelinovsky, E., Yalciner, A., Kurkin, A., Kozelkov, A., Zaitsev, A., 2003b. The 1876 Virgin Isdland Tsunami: Observation and Modeling. Oceanologica Acta. 26, 609 – 621.

Table 1. Computed maximum water levels

| | Highest of maximum elevation (m) | Maximum elevation around Phuket (m) | Maximum elevation around Penang Island (m) |
|---|---|---|---|
| ED(1) | 12.09 | 4.03 – 10.48 | 1.6 – 3.2 |
| BC-ED(1) | 14.15 | 4.7 – 11.3 | 1.8 – 3.7 |
| BC-ED(1) (adjusted) | 12.26 | 3.6 – 9.8 | 1.6 – 2.5 |
| ED(2) | 11.82 | 3.74–10.24 | 1.57–2.36 |
| BC-ED(2) | 14.01 | 3.9–12.14 | 1.8–2.8 |
| BC-ED(2) (adjusted) | 11.85 | 3.1–10.27 | 1.5–2.3 |
| ED(3) | 8.87 | 3.5–8.2 | 1.1–1.8 |
| BC-ED(3) | 13.36 | 3.7–10.6 | 1.7–3.02 |
| BC-ED(3) (adjusted) | 9.26 | 2.8–8.02 | 1.2–2.4 |

Table2. The scale factor for the amplitude due to the response of the sources in different distances.

| Distance of the source from it original position (in km) | Value of the scale factor ($s'$) |
|---|---|
| 1100 | 0.85 |
| 1500 | 0.85 |
| 2500 | 0.80 |
| 3200 | 0.75 |
| 4500 | 0.70 |

Manuscript received Sep. 14, 2007; revised Mar. 20, 2008


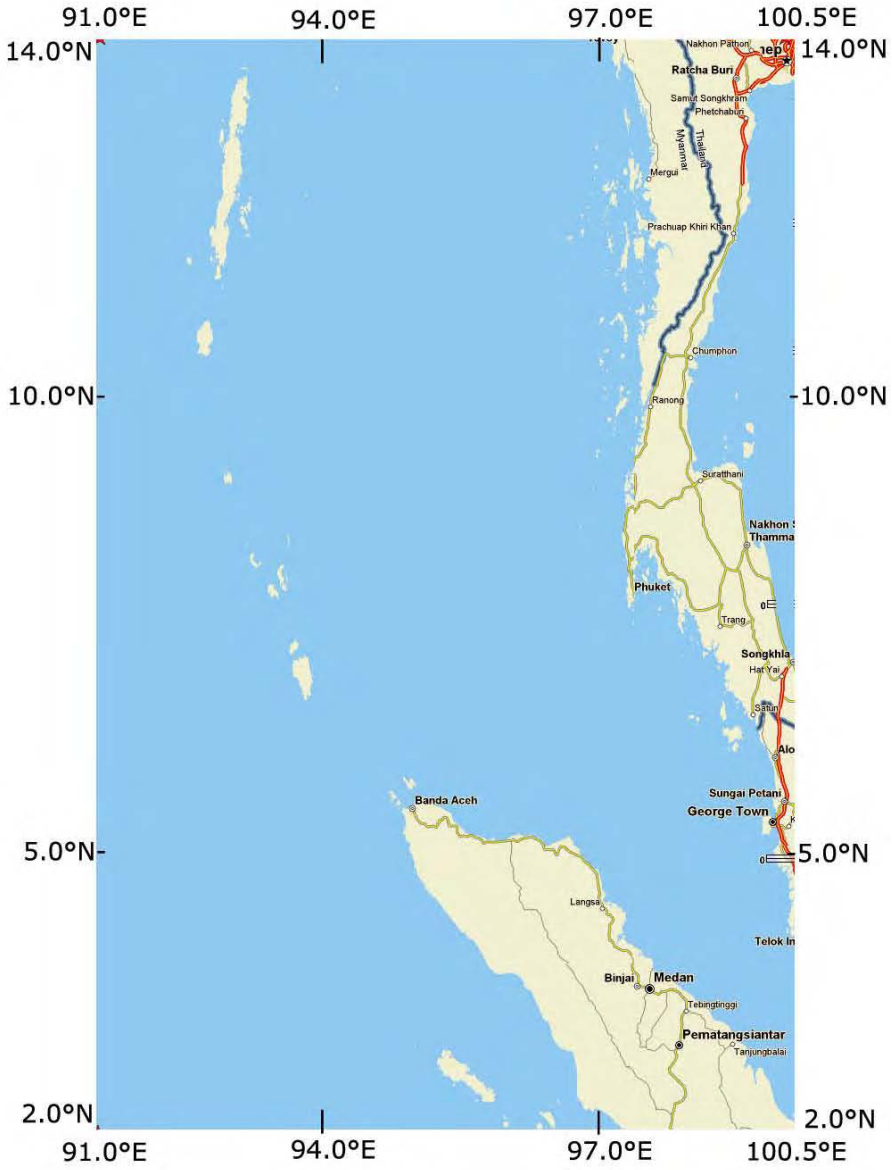


Figure 1: The original model domain (OD).

Manuscript received Sep. 14, 2007; revised Mar. 20, 2008


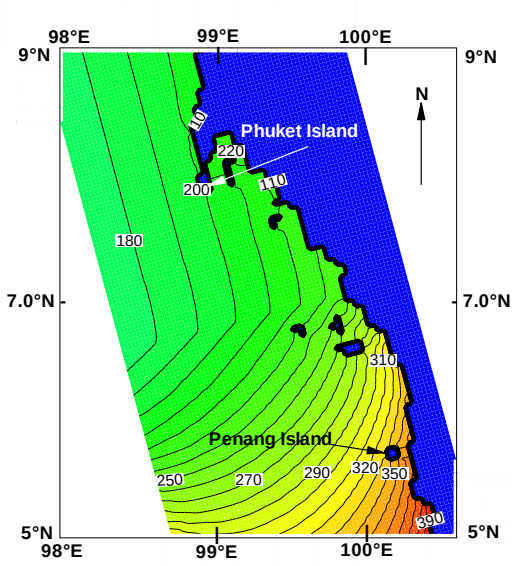


Figure 2: Tsunami propagation time in minutes towards Phuket and Penang Island due to source in ED(1).

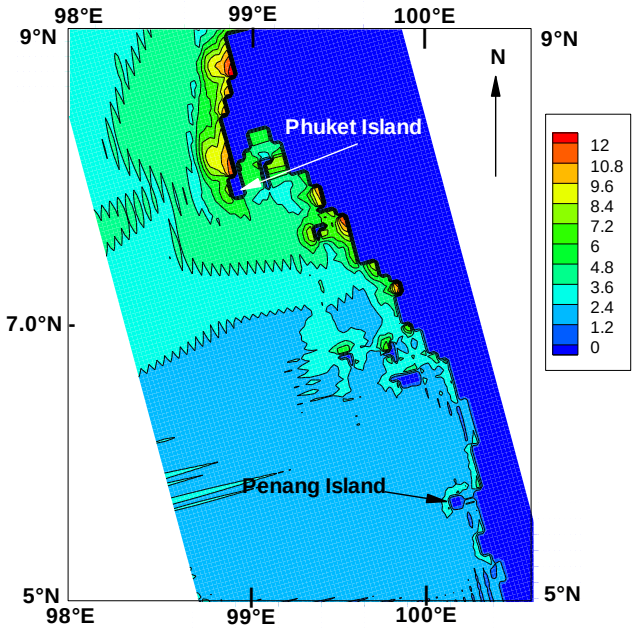


Figure3. Maximum elevation due source in ED(1) around the west coast of Thailand and Malaysia.

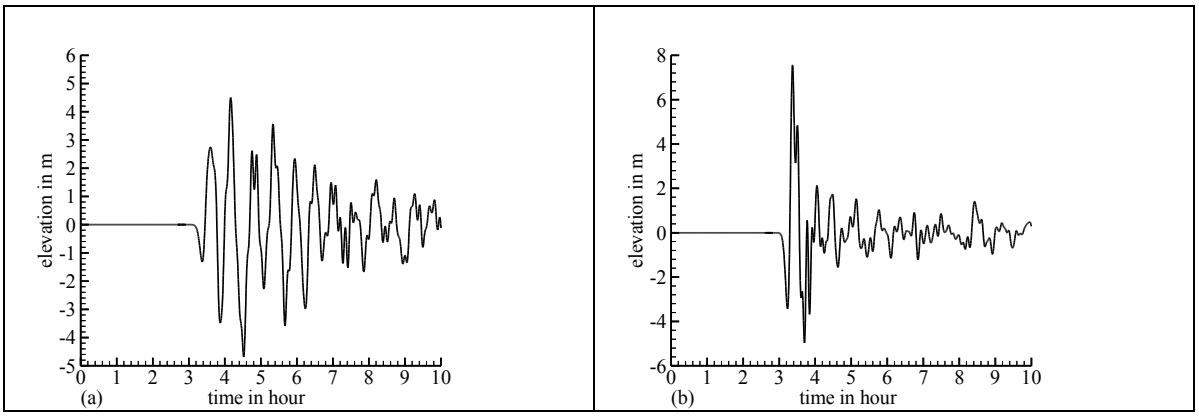


Figure 4: Computed water level fluctuation at two coastal locations of Phuket Island associated with the source in ED(1): (a) East Phuket, (b) South-west Phuket.

Manuscript received Sep. 14, 2007; revised Mar. 20, 2008


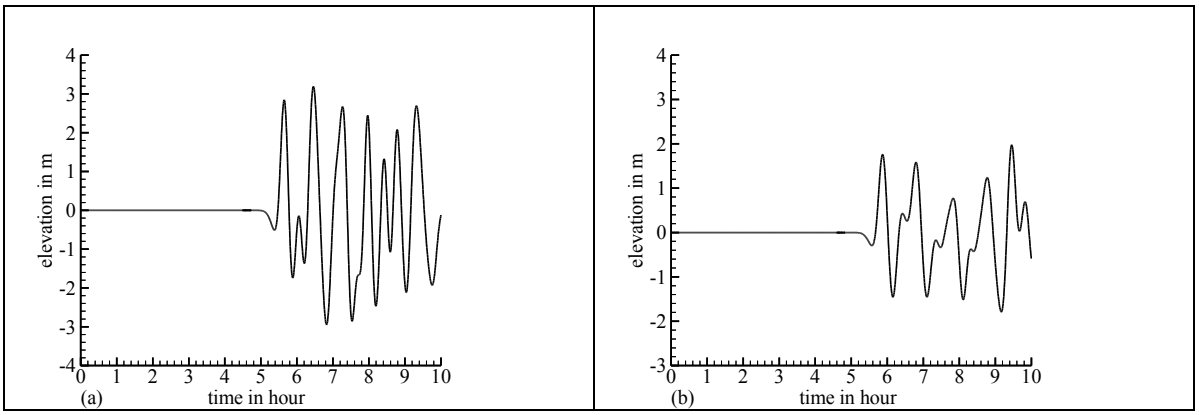


Figure 5: Computed water level fluctuation at two coastal locations of Penang Island associated with the source in ED(1):: (a) Batu Ferringi, (b) South coast.

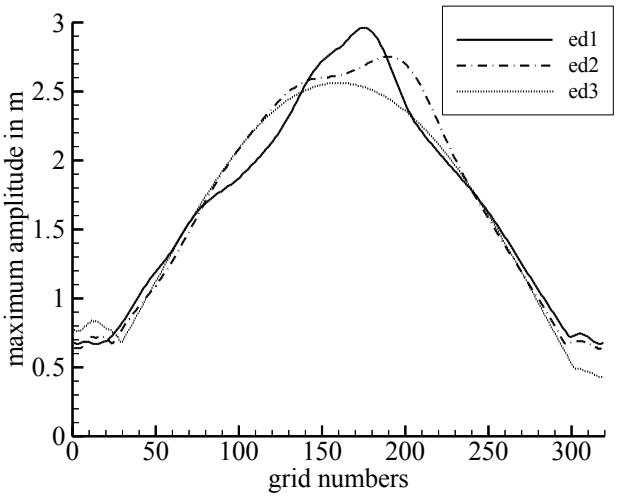


Figure 6: Maximum amplitudes of the tsunami waves at the west open boundary of OD due to the sources in ED($i$), $i$ = 1, 2, 3.

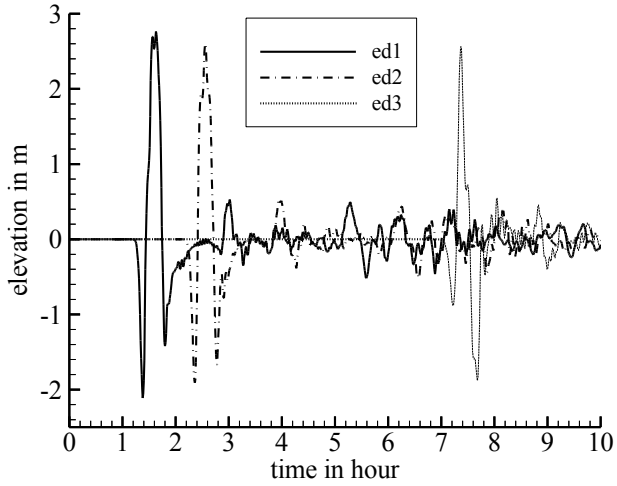


Figure 7: Computed water level fluctuation at a point on the open boundary of OD due to the sources in ED($i$), $i$ = 1, 2, 3.

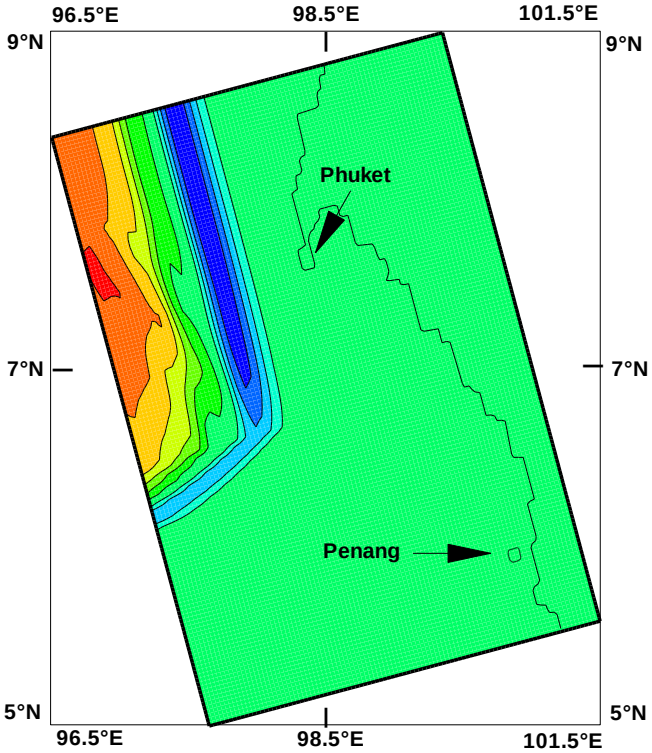


Figure 8a: Computed tsunami disturbance pattern at 1.5 hr.

Manuscript received Sep. 14, 2007; revised Mar. 20, 2008


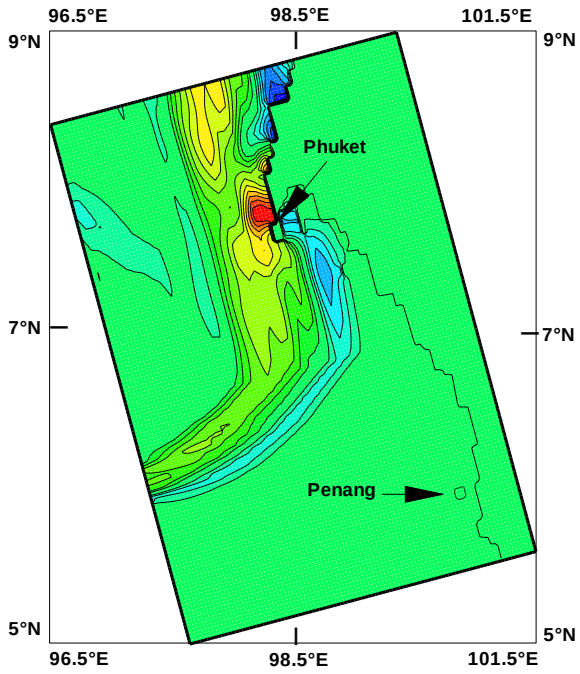


Figure 8b: Computed tsunami disturbance pattern at 2 hr.

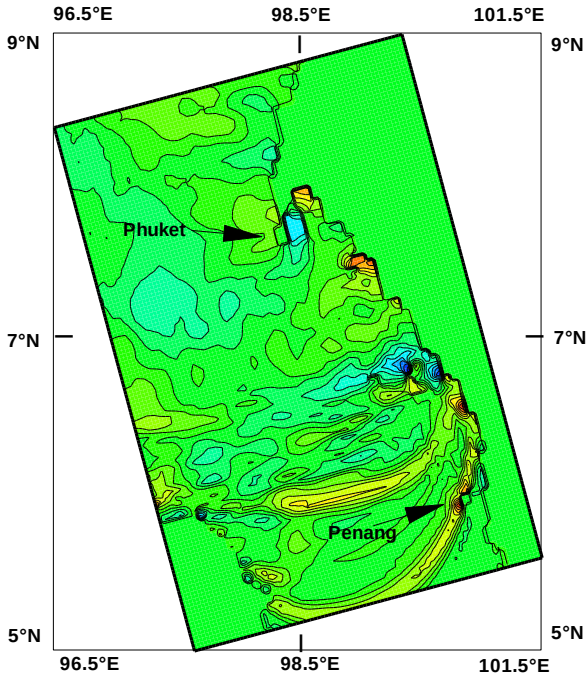


Figure 8d: Computed tsunami disturbance pattern at 4.7 hr.

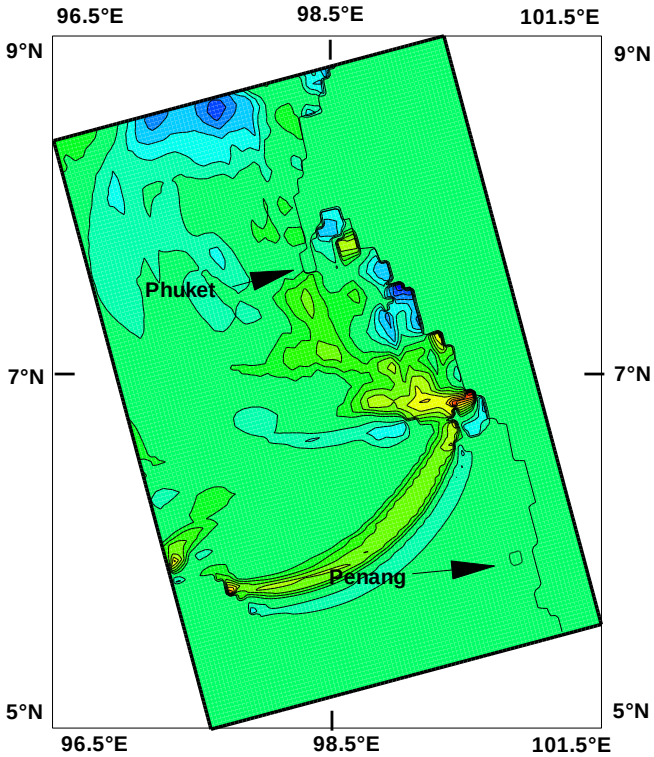


Figure 8c: Computed tsunami disturbance pattern at 3.5 hr.

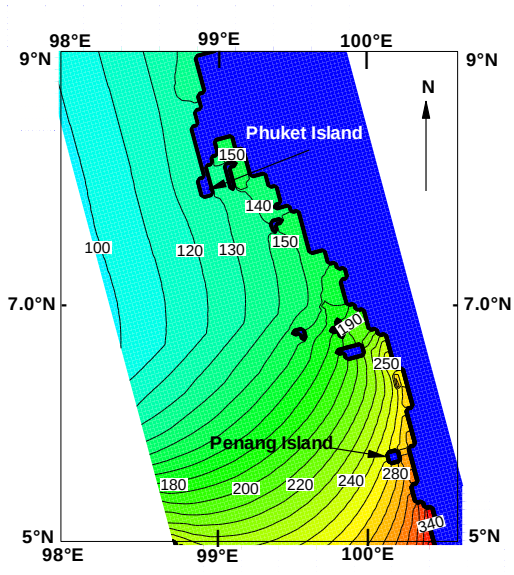


Figure 9: Tsunami propagation time in minutes towards Phuket and Penang Island due to BC-ED(1).

Manuscript received Sep. 14, 2007; revised Mar. 20, 2008


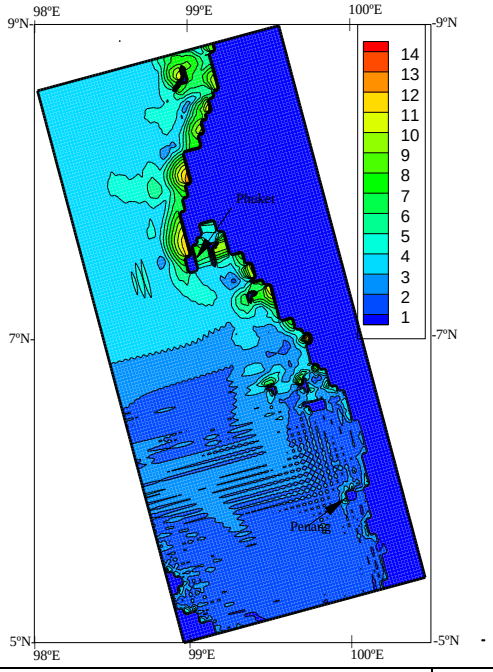


Figure 10: Maximum elevation due to BC-ED(1) around the west coast of Thailand and Malaysia.

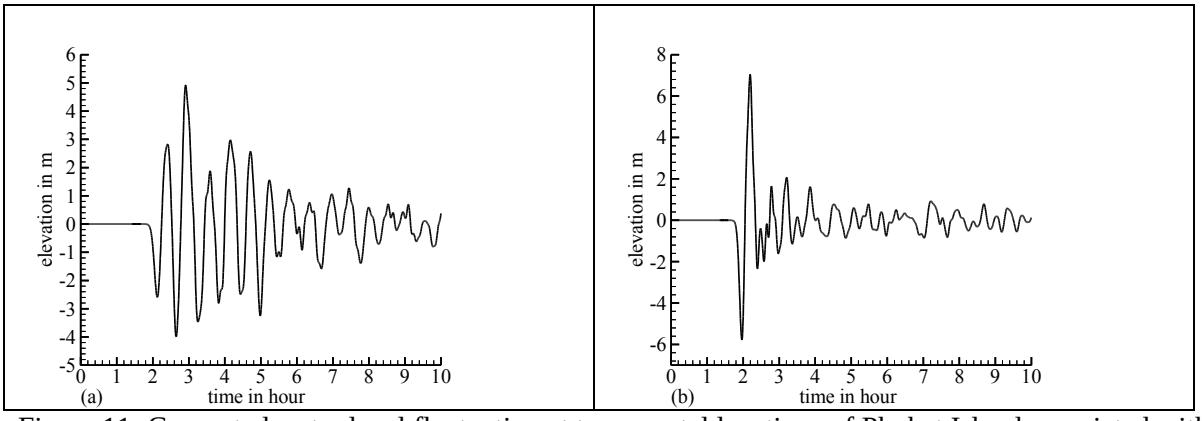


Figure 11: Computed water level fluctuation at two coastal locations of Phuket Island associated with BC-ED(1): (a) East Phuket, (b) South-west Phuket.

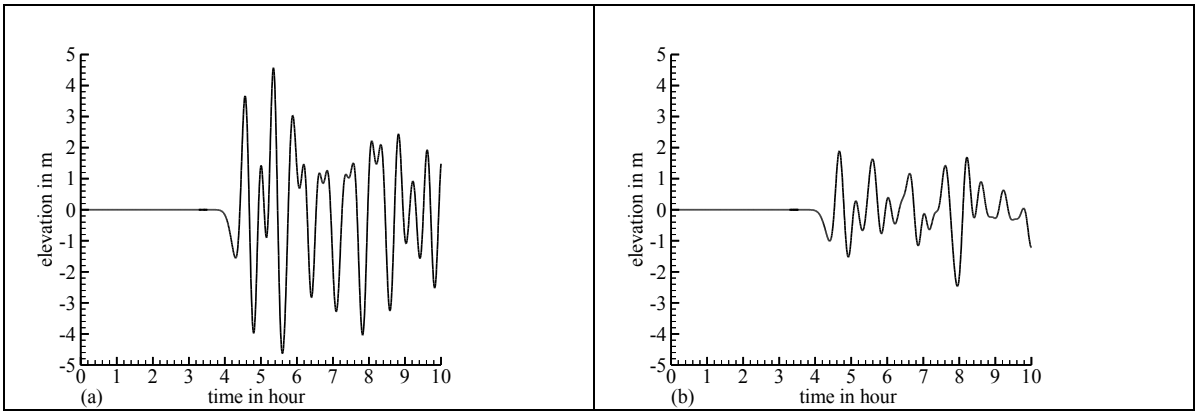


Figure 12: Computed water level fluctuation at two coastal locations of Penang Island associated with BC-ED(1): (a) Batu Ferringi (north coast), (b) South coast.

Manuscript received Sep. 14, 2007; revised Mar. 20, 2008


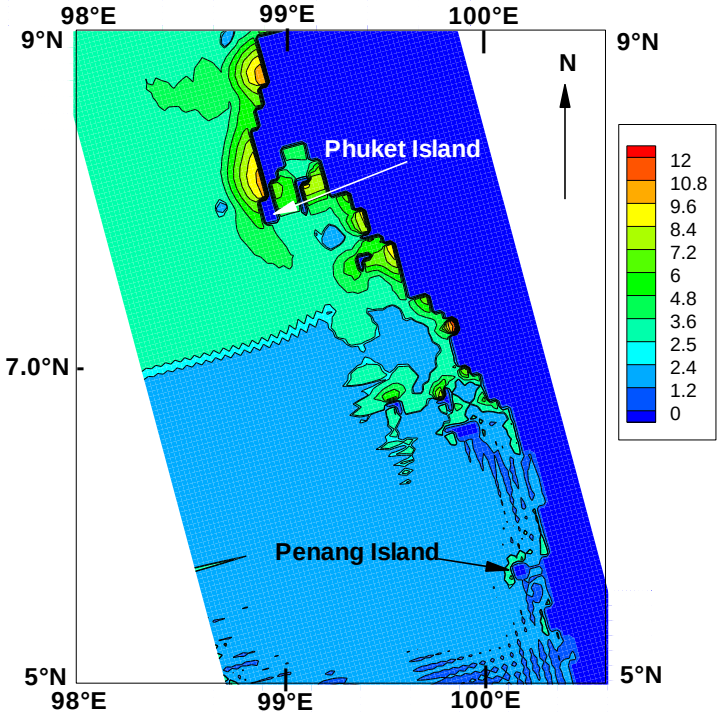


Figure 13: Maximum elevation due to BC-ED(1), with adjusted amplitude, around the west coast of Thailand and Malaysia.

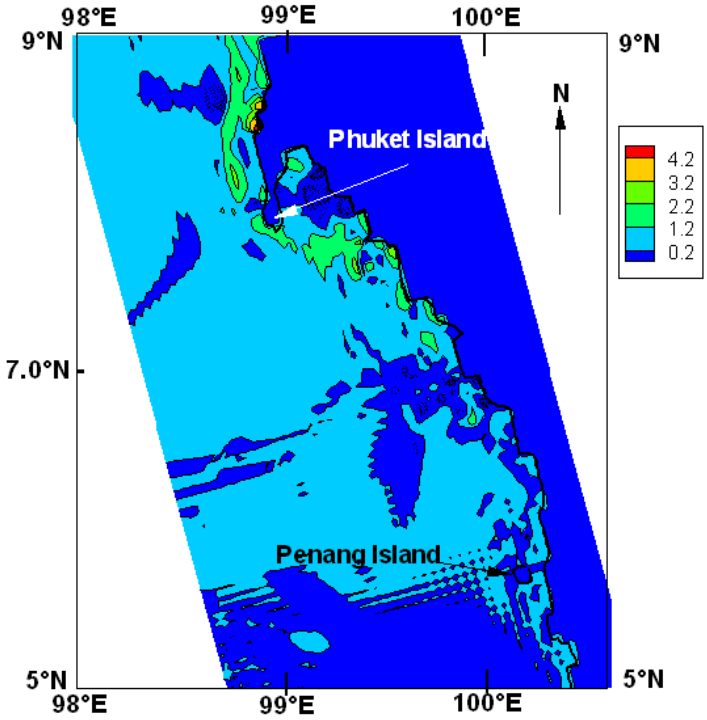


Figure 14: Anomaly of maximum elevations around the west coast of Thailand and Malaysia associated with the source in ED(1) and BC-ED(1) with adjusted amplitude